value at $r_{max} > r_e$ if $r_{min}(\psi_2) > r_e$, where $r_{min}(\psi_2)$ is the energy minimum C–X distance of the ionic configuration ψ_2. Since we show by ab initio calculations that $r_{max} > r_e$ for a number of MeX systems, it can be concluded that $r_{min}(\psi_2)$ is greater than r_e for those systems.[8a] This situation arises from a subtle interplay between the energy gap (Δ) between ψ_1 and ψ_2, and the exchange matrix element (U_{12}) which couples ψ_1 and ψ_2, in separately determining r_e and r_{max}.

The r_{max}/r_e vs BDE correlation can also be explained by the VB model. To a crude approximation it can be assumed that (on a normalized r_{C-X}/r_e scale), for a given rightward displacement (to larger r_{C-X}) from the equilibrium geometry, the U_{12} term for configuration mixing, which is similar to the Me–X overlap term, will be nearly the same regardless of the identity of X. Therefore, the contribution of U_{12} to the configuration mixing and the resulting ionicity will be roughly independent of X at a given r_{C-X}/r_e. On the other hand, because the energy gap (Δ) in the bonding region roughly parallels the BDE value as a function of X, it will tend to induce relatively more configuration mixing for a MeX system with a greater BDE at larger r_{C-X}/r_e values where Δ is smaller. In contrast, for a MeX system with a weaker bond (smaller BDE), the energy gap will vary less steeply with r_{C-X}/r_e (see Figure 3). Consequently, the maximum ionicity for large BDE methyl derivatives will be shifted more to the right, thus approximately giving the dependence of r_{max}/r_e on the BDE shown in Figure 2.

To the best of our knowledge, this is the first rigorous study which demonstrates that the electronic structure on the reaction path leading from reactants to products may not have features intermediate between the species at the two ends of the reaction profile. This also seems to be the first observation of the ionicity oscillation phenomenon for a reaction of such general nature as the homolysis of C–X bonds. The implications of these results to the interpretation of LFER are rather straightforward. Let us assume that a hypothetical reaction of this nature has a TS which can be probed by substituents on the methyl group.[9] If these substituents are designed to measure atom or group charges (via rho values or any equivalent reaction parameter), the traditional expectation would be that, since in the course of the reaction the methyl group monotonically loses its positive charge, the measured rho value will be larger as the TS comes later, reflecting the larger charge loss from the Me group. However, using the example in Figure 2 for MeOH and assuming that in this hypothetical reaction a TS is located around $r = 2.3$ Å, the measured rho value will be small because the polarity at this r_{C-O} value is about the same as that of the reactant at its equilibrium geometry. The inferred conclusion would then be that the TS resembles the reactants, i.e., is achieved early. In the absence of other evidence to the contrary, this erroneous conclusion would be widely accepted, since the experimental results do not contradict the assumption that the TS is of intermediate nature between (i.e., bound by) the reactants and products. The error in this assumption will be recognized only if the TS has an ionicity *larger* than that of the GS (e.g., around $r = 1.8$ Å in Figure 1). In this case, the unusual behavior of the system will be recognized as such due to the "wrong" sign of the measured rho value. It should be noted that when the reaction is viewed from the reverse direction the rho value will always have the "right" sign. However, as in the specific example of Figure 1 at $r = 1.8$ Å, its absolute value will exceed the equilibrium value somewhere along the association reaction path. This latter phenomenon has recently been discussed[10] in terms of a three VB configuration model.

The observation that along the reaction path for such an elementary reaction as a single-step homolytic dissociation the property value boundaries set by reactants and products can be exceeded suggests that the observed phenomenon is of a general nature. The traditional interpretation of rho values in terms of an early or late location of the TS should therefore be checked by independent experimental evidence for consistency.

Registry No. CH_3CN, 75-05-8; $CH_3C{\equiv}CH$, 74-99-7; $CH_3CH{=}CH_2$, 115-07-1; CH_3F, 593-53-3; CH_3OH, 67-56-1; CH_3NH_2, 74-89-5; CH_3NO_2, 75-52-5; CH_3N_3, 624-90-8; CH_3NO, 865-40-7.

Supplementary Material Available: Figure showing variations of energy and dipole moment as a function of r_{C-O} and a table of the related data for the dissociation of MeOH (2 pages). Ordering information is given on any current masthead page.

(9) An actual TS can be found in homolytic dissociations of this type in cases where the odd electron in the bonding σ orbital on X relaxes during the dissociation process to a lower energy orbital (i.e., $CH_3{:}NC \rightarrow CH_3^{\bullet} + NC^{\bullet}$).

(10) Pross, A.; Shaik, S. S. *J. Am. Chem. Soc.* **1982**, *104*, 1129.

Stacked or T-Shaped Benzene Dimer in Aqueous Solution? A Molecular Dynamics Study

Per Linse

Contribution from Physical Chemistry 1, Chemical Center, University of Lund, P.O. Box 124, S-221 00 Lund, Sweden. *Received July 22, 1991*

Abstract: An aqueous solution of a benzene dimer has been investigated by means of molecular dynamics simulations. The potential of mean force as a function of the benzene separation for stacked and T-shaped configurations has been calculated. The close-contact T-shaped dimer was found to possess the lowest free energy. The more favorable benzene–benzene and benzene–water interaction present for the T-shaped geometry exceeds the increase in the hydrophobic surface free energy as compared to the close-contact stacked dimer. Moreover, a well-defined solvent-separated stacked minimum with a similar potential of mean force as the close-contact stacked minimum was obtained. The hydration of the benzene dimer is very similar to that of a single benzene molecule. The main exception occurs for the solvent-separated stacked dimer where water molecules located between the benzene dimer display a weaker preferential orientation with respect to the benzene molecules and a moderately enhanced water structure.

Introduction

There is experimental evidence that a small fraction of the benzene molecules dissolved in water occurs as dimers,[1] but information on the dimer structure is lacking. However, there are experimental data indicating that the planes of benzene in the dimer are not parallel in the gas phase,[2-4] and similar perpendicular

(1) Tucker, E. E.; Lane, E. H.; Christian, S. D. *J. Solution Chem.* **1981**, *10*, 1.

(2) Janda, K. C.; Hemminger, J. C.; Winn, J. S.; Novick, S. E.; Harris, S. J.; Klemperer, W. *J. Chem. Phys.* **1975**, *63*, 1419.

(3) Steed, J. M.; Dixon, T. A.; Klemperer, W. *J. Chem. Phys.* **1979**, *70*, 4940.

0002-7863/92/1514-4366$03.00/0

or close perpendicular arrangements are frequently found among neighbors in crystalline benzene.[5] In proteins, it is also found that the probability of the stacked (also referred to as the face-to-face) arrangement is suppressed,[6-9] and that arrangements with attractive benzene–benzene interaction play a significant role in the stability of proteins.[10]

Hydrophobic substances dissolved in aqueous media tend to minimize their area exposed toward the solvent. The smaller area exposed by the stacked benzene dimer, as compared to the T-shaped dimer, should favor the stacked configuration in the presence of an aqueous medium. On the other hand, benzene possesses a permanent charge distribution of which a significant quadrupole moment is the first nonzero term in an electrostatic multipole expansion. The most important electrostatic interaction between benzene molecules, the quadrupole–quadrupole interaction, is attractive for the T-shaped dimer, whereas it is repulsive for the stacked dimer.[11,12] Hence, the two arrangements selected represent two extremes: one minimizing the area exposed and the other minimizing the direct benzene–benzene interaction energy. In aqueous solution, the following question arises: which effect dominates, the hydrophobic one which favors the stacked dimer or the direct benzene–benzene interaction which favors a T-shaped dimer? However, beside this simple picture, in the last decade simulation studies unambiguously indicate that solvent-separated configurations are frequently populated. Hence, we have not only to consider close-contact configurations, but also solvent-separated ones.

Earlier molecular simulation studies of the benzene dimer in water solution have only partly addressed this issue. Ravishanker and Beveridge[13] have investigated the stacked arrangement only, whereas Jorgensen and Severance[14] studied an orientationally averaged dimer. Thus, both investigations have left the question of the most favorable benzene dimer in aqueous solution essentially unanswered, although the latter study showed that the close-contact stacked arrangement is infrequent.

In this study the benzene dimer in aqueous solution is examined by means of molecular dynamics (MD) simulation. Calculations of the potential of mean force (pmf) as a function of the benzene separation and orientation have been carried out. The difference in the pmf between two benzene arrangements is the reversible work required to transform one of them into the other. The work may be divided into two constituents: one arising from the direct benzene–benzene interaction and one from the presence of the solvent. The latter, frequently referred to as the cavity or the solvent contribution, requires complete averages of the configurational space of the solvent molecules for numerous arrangements of the benzene dimer and thus involves a significant computational effort.

In addition to the pmf calculations, the hydration structure of some selected benzene arrangements is investigated and related to the structure of a single hydrated benzene molecule.[15]

Model System and Simulation Methodology

Molecular dynamics simulations were carried out on a model system consisting of two benzene and 500 water molecules. All interactions were evaluated explicitly assuming pairwise additivity and all molecules were kept rigid. The benzene–benzene and the benzene–water intermolecular potential energies used were obtained from ab initio quantum chemical calculations using the Hartree–Fock self-consistent field approximation, and the dispersion energy contribution was obtained by a perturbation procedure.[11] The TIP4P[16] potential energy function was used for the water–water interaction. The benzene–water and water–water potentials have previously been used in molecular dynamics simulation of a dilute aqueous solution of benzene[15] and gave improved results over previous similar investigations.[17,18] The benzene–benzene potential has been employed in our laboratory for investigations of liquid benzene[19,20] as well as of a liquid–liquid benzene–water interface.[21]

The MD simulations were performed with the MOLSIM package.[22] Newton's equations of motion were integrated using the velocity form of the Verlet algorithm with a time step of 1.0 fs, and the orientations of the rigid molecules were described in a quaternion representation.[23] The simulation box was a parallelepiped with edges approximate 22 × 22 × 32 Å. The benzene dimer was held fixed and placed along the long-axis of the box (one exception) with their common center-of-mass at the origin of the external coordinate frame. Periodical boundary conditions were used together with a spherical molecular cutoff of 10.0 Å and a neighbor list technique with an automatic check of the update interval. All interactions were evaluated from a look-up table, and a quadratic interpolation scheme was also used. The temperature and the pressure were kept constant by using 298 K and 0.103 MPa as external values and applying a scaling procedure developed by Berendsen et al.[24] with time constants of 0.1 ps.

Two sets of simulations have been performed. The first one comprises calculation of the pmf as a function of the benzene separation for a stacked and a T-shaped benzene dimer as well as a direct determination of the difference in the pmf between the close-contact stacked and the close-contact T-shaped configuration. In the stacked geometry, the C_6 axis of each molecule superimposes the intermolecular benzene–benzene vector, whereas in the T-shaped geometry one of the C_6 axis is turned to be perpendicular to the intermolecular vector. The second set involves determination of the hydration structure of close-contact and solvent-separated benzene dimers.

The two pmf functions with fixed benzene orientations were obtained from 13 and 12 simulations, respectively, where each simulation comprised 18 ps averaging, whereas the last pmf function consisted of 11 points, each 9 ps. The hydration structures were determined from simulations covering 36 ps for each benzene arrangement studied. The simulations were performed on IBM 3090-170S VF and 3090-600J VF computers, and one time step required 4.8 and 3.0 CPU s, respectively.

The free energy difference between two benzene configurations, and in more general terms two states, can be computed by using thermodynamic perturbation theory.[25] In this context it is useful to consider the benzene dimer as a "supermolecule" since the configurational average is taken for a fixed benzene configuration. Hence, in this section it is natural to refer to benzene states rather than to benzene configurations. Within the perturbation formalism, the free energy difference between the perturbed and the reference state is given by

(4) Börnsen, K. O.; Selzle, H. L.; Schlag, E. W. *J. Chem. Phys.* **1986**, *85*, 1726.
(5) Cox, E. G.; Cruickshank, D. W. J.; Smith, J. A. S. *Proc. R. Soc. London, Ser. A* **1958**, *247*, 1.
(6) Burley, S. K.; Petsko, G. A. *Science* **1985**, *229*, 23.
(7) Singh, J.; Thornton, J. M. *FEBS Lett.* **1985**, *191*, 1.
(8) Blundell, T.; Singh, J.; Thornton, J.; Burley, S. K.; Petsko, G. A. *Science* **1986**, *234*, 1005.
(9) Burley, S. K.; Petsko, G. A. *Adv. Protein Chem.* **1988**, *39*, 125.
(10) Serrano, L.; Bycroft, M.; Fersht, A. R. *J. Mol. Biol.* **1991**, *218*, 465.
(11) Karlström, G.; Linse, P.; Wallqvist, A.; Jönsson, B. *J. Am. Chem. Soc.* **1983**, *105*, 3777.
(12) Hobza, P.; Selzle, H. L.; Schlag, E. W. *J. Chem. Phys.* **1990**, *93*, 5893.
(13) Ravishanker, G.; Beveridge, D. L. *J. Am. Chem. Soc.* **1985**, *107*, 2565.
(14) Jorgensen, W. L.; Severance, D. L. *J. Am. Chem. Soc.* **1990**, *112*, 4768.
(15) Linse, P. *J. Am. Chem. Soc.* **1990**, *112*, 1744.
(16) Jorgensen, W. L.; Chandrasekhar, J.; Madura, J. D.; Impey, R. W.; Klein, M. L. *J. Chem. Phys.* **1983**, *79*, 926.
(17) Linse, P.; Karlström, G.; Jönsson, B. *J. Am. Chem. Soc.* **1984**, *106*, 4096.
(18) Ravishanker, G.; Mehrotra, P. K.; Mezei, M.; Beveridge, D. L. *J. Am. Chem. Soc.* **1984**, *106*, 4102.
(19) Linse, P. *J. Am. Chem. Soc.* **1984**, *106*, 5425.
(20) Linse, P.; Engström, S.; Jönsson, B. *Chem. Phys. Lett.* **1985**, *115*, 95.
(21) Linse, P. *J. Chem. Phys.* **1987**, *86*, 4177.
(22) MOLSIM 1.1: Linse, P., University of Lund, Sweden, 1990.
(23) Allen, M. P.; Tildesley, D. J. *Computer Simulation of Liquids*; Oxford University Press: Oxford, 1987.
(24) Berendsen, H. J. C.; Postma, J. P. M.; Gunsteren, v. W. F.; Dinola, A.; Haak, J. R. *J. Chem. Phys.* **1984**, *81*, 3684.
(25) Zwanzig, R. W. *J. Chem. Phys.* **1954**, *22*, 1420.

$$\Delta G \equiv G_1 - G_0 = -RT \ln \langle e^{-\Delta U/RT} \rangle_0 \quad (1)$$

where $\Delta U \equiv U_1 - U_0$ is the difference between the potential energy functions of the perturbed state U_1 and reference state U_0. The symbol $\langle ... \rangle_0$ denotes an average using an equilibrium ensemble representative for the reference state, R the molar gas constant, and T the temperature. Although eq 1 is exact, it is computationally feasible only if the equilibrium ensembles of the reference and the perturbed states are not too different. A guideline often used is that ΔG should not exceed a few times RT.[26] As previously mentioned,[27] this is not a sufficient condition, since ΔG might be small *even if* the equilibrium ensemble of the reference state is *not* representative for the perturbed state.

If the perturbation is large, we have to introduce (physical or nonphysical) intermediate states and to calculate the free energy difference between adjacent states, ΔG_i. Since the free energy is a state function, the total free energy ΔG follows from

$$\Delta G = \sum_{i=1}^{N-1} \Delta G_i \quad (2)$$

The intermediate and end states are specified by the discrete variable λ. The reference state is given by $\lambda_1 = 0$ and the fully perturbed state by $\lambda_N = 1$, whereas the intermediate $N - 2$ states are given by $0 < \lambda_i < 1$, $i = 2, 3, ..., N - 1$. The free energy difference between state λ_{i+1} and λ_i is given by

$$\Delta G_i = -RT \ln \langle e^{-\Delta U_i/RT} \rangle_{\lambda_i} \quad (3)$$

where $\Delta U_i \equiv U_{\lambda_{i+1}} - U_{\lambda_i}$ is the difference in the potential energy function of the two states.

The change of λ from 0 to 1 will map the path for which the pmf will be calculated. For a spacial perturbation linear in λ, the intermediate states can be expressed as

$$\mathbf{R}(\lambda) = \mathbf{R}_0 + \lambda(\mathbf{R}_1 - \mathbf{R}_0) \quad (4)$$

where $\mathbf{R}_0$ denotes the initial and $\mathbf{R}_1$ the final benzene state with $\mathbf{R} \equiv \{\mathbf{r},\Omega\}$, $\mathbf{r}$ the benzene–benzene intermolecular vector, and Ω the three orientational degrees of freedom, e.g., the Euler angles. In the two cases of fixed relative benzene orientations, parallel (stacked) and perpendicular (T-shaped), eq 4 reduces to

$$r(\lambda) = r_0 + \lambda(r_1 - r_0) \quad (5)$$

where r is the intermolecular center-of-mass separation. The lower ends used were 3.1 and 4.3 Å and the upper ones 7.9 and 8.7 Å, respectively. The difference in benzene–benzene separation between subsequent states was in both cases $\Delta r = 0.4$ Å. Since for each intermediate state a free energy difference can be evaluated for a perturbation in either direction (smaller or larger λ), free energy differences are evaluated for states separated by $\Delta r = 0.2$ Å. Finally, both benzene molecules were perturbed by an equal amount; thus each molecule was displaced 0.1 Å in the two first perturbation calculations. The third pmf computation comprised a simultaneous translation and rotation from a parallel orientation at $r = 3.5$ Å to a perpendicular orientation at $r = 4.7$ Å. These separations correspoond to the close-contact minima of the two pmf functions (see below). The separation as well as the orientation (a single Euler angle in the present case) was linearly changed among the nine intermediate states, and both molecules were equally displaced 0.06 Å and rotated 2.25°.[28]

For the investigation of the effect of the water on the pmf, it is useful to define the solvent contribution. It is obtained by subtracting the benzene–benzene pair energy, $U_{BB}(\mathbf{R})$, from the pmf, $w(\mathbf{R})$, according to

$$w_s(\mathbf{R}) = w(\mathbf{R}) - U_{BB}(\mathbf{R}) \quad (6)$$

(26) Beveridgde, D. L.; DiCaputa, F. M. *Computer Simulation of Biomolecular Systems. Theoretical and Experimental Applications*; van Gunsteren, W. F., Weiner, P. K., Eds.; Escom: Leiden, The Netherlands, 1989.
(27) Straatsma, T. P.; McCammon, J. A. *J. Chem. Phys.* **1989**, *90*, 3300.
(28) Since both benzene molecules were rotated, they had to be translated off their interparticle axis (and hence also off the long-axis of the box).

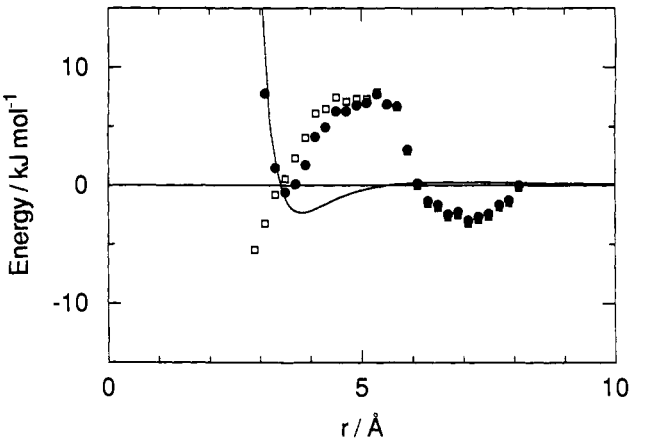

Figure 1. Potential of mean force, $w(r)$ (filled circles), the benzene–benzene potential energy, $U_{BB}(r)$ (solid curve), and the solvent contribution to the potential of mean force, $w_s(r) = w(r) - U_{BB}(r)$ (open squares), for the stacked benzene dimer as a function of the benzene–benzene separation. The potential of mean force function and its solvent contribution contain a common undetermined additive energy constant.

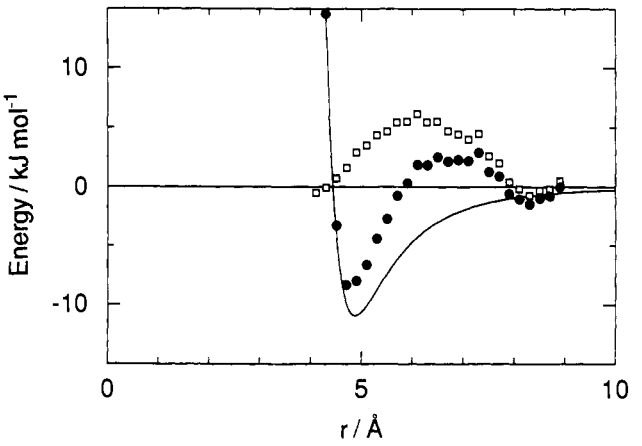

Figure 2. Same as Figure 1, but for the T-shaped benzene dimer.

The solvent term contains contributions from both benzene–water and water–water interactions and is zero in the gas phase. The solvent contribution will be related to the total area available for water molecules in the primary hydration shell of the benzene dimer. The area was calculated by using a van der Waals radius of 1.7 Å for the carbon atoms and a probe radius of 1.4 Å, which reasonably reproduces the surface where the benzene–water pair potential is zero.

The statistical uncertainties of quantities related to the pmf reported are one standard deviation and they are based on a division of a simulation into 1-ps segments. The extended simulation of each state and the small displacements resulted in high accuracy. The mean uncertainties of the difference in the pmf for adjacent points were 0.3, 0.2, and 0.3 kJ mol^{-1} for the stacked dimer, T-shaped dimer, and stacked to T-shaped transition, respectively. Assuming independent errors, the uncertainty of the free energy difference for two benzene dimers with a *difference in separation* of d Å becomes $0.7(d)^{1/2}$ and $0.5(d)^{1/2}$ kJ mol^{-1} Å$^{-1/2}$ for the stacked and the T-shaped dimer, respectively. With the same assumption, the uncertainty of the free energy difference between the close-contact stacked and close-contact T-shaped geometries is 1.3 kJ mol^{-1}. The uncertainties reported for the structural quantities are also one standard deviation but based on 3-ps segments.

Beside the statistical uncertainties, there is also a systematic error of the pmf functions at large separations due to the fact that the separation becomes close to the potential cutoff. It is difficult to determine this error from the present investigation only, but the use of the third pmf function indicates that this effect is limited (see below).

Table I. Difference in Potential of Mean Force and Related Quantities[a]

transition							
geometry	r_0	r_1	Δw	ΔU_{BB}	Δw_s	Δarea	ΔU_{BW}
			Close-Contact to Solvent-Separated				
stacked	3.5	7.1	−2.4 ± 1.3	+1.4	−3.8 ± 1.3	110	−21 ± 3
T-shaped	4.7	8.3	+6.8 ± 0.9	+9.1	−2.3 ± 0.9	84	−14 ± 3
			Stacked to T-Shaped				
close-contact	3.5	4.7	−10.4 ± 1.3	−8.8	−1.6 ± 1.3	26	−16 ± 3
			Close-Contact to Transition State				
stacked	3.5	5.3	+8.3 ± 0.9	+1.0	+7.3 ± 0.9		
T-shaped	4.7	6.5	+10.8 ± 0.7	+6.9	+3.9 ± 0.7		
			Solvent-Separated to Transition State				
stacked	7.1	5.3	+10.7 ± 0.9	−0.4	+11.1 ± 0.9		
T-shaped	8.3	6.5	+4.0 ± 0.7	−2.2	+6.2 ± 0.7		

[a] r_0 and r_1 denote the center-of-mass separations of the benzene dimer; $\Delta w(\equiv w_1 - w_0)$ is the difference in potential of mean force; ΔU_{BB} difference in benzene interaction; $\Delta w_s \equiv \Delta w - \Delta U_{BB}$, difference in solvent contribution; Δarea difference in area available for water molecules; and ΔU_{BW} difference in the ensemble average of the total benzene–water interaction energy. Energies are in kJ mol^{-1}, lengths in Å, and area in Å^2. Uncertainties given are one standard deviation (see text).

Results and Discussion

Potential of Mean Force. Figures 1 and 2 show the calculated pmf functions employing eqs 2, 3, and 5 for the stacked and T-shaped benzene dimer. Included in the figures are the benzene–benzene potential energy functions and also the resulting solvent contributions. The pmf functions and hence their solvent contributions contain an undetermined additive energy constant since only relative free energies are obtained. The functions level off at increased separations, and they are normally defined to be zero at infinite separation. In the present investigation, the pmf's were set to zero at the largest distances used, 8.1 and 8.9 Å, respectively. By employing a larger system and an increased cutoff, the tails of the pmf functions and their energy scales could be determined more accurately. Here, the two pmf functions were *rigorously* connected by the direct determination of the difference in the pmf between the close-contact stacked and the close-contact T-shaped configuration. The free energy difference between the upper endpoints of the pmf functions in Figures 1 and 2 became 1.9 kJ mol^{-1}, which is smaller than the overall estimated uncertainty, 2.2 kJ mol^{-1}, and hence indicates that the values at the upper endpoints are not far from their values at infinite separation and that the effect of the potential cutoff is limited. Nevertheless, our main interest will be devoted to the free energy changes at smaller separations, and they are independent of the pmf functions at large separations.

It is obvious from Figure 1 that the pmf function of the stacked dimer possesses two minima. The one at r = 3.5 Å will be referred to as the *close-contact* and the one at r = 7.1 Å as the *solvent-separated* minimum. The minima have similar free energies (cf. Table I), and there is an appreciable energy barrier of ≈9 kJ mol^{-1} in between. On the contrary, Figure 2 shows that, for the T-shaped dimer, the close-contact geometry has the far lowest free energy, 7 kJ mol^{-1} lower than the solvent-separated dimer. Moreover, the barrier for achieving a close-contact T-shaped dimer from the solvent-separated one is only a third of that for a stacked dimer (cf. Table I). By comparing the two pmf functions in Figures 1 and 2, we can readily conclude that, of the dimers studied, the close-contact T-shaped dimer has the lowest free energy and is ≈6 kJ mol^{-1} below the solvent-separated stacked dimer.[29]

The direct benzene–benzene interactions of the two geometries differ substantially. For the stacked benzene dimer, the repulsive quadrupole–quadrupole interaction almost cancels the attractive dispersion interaction, giving only a weak attraction at small separation (see Figure 1). On the other hand, the T-shaped dimer displays a energy minimum of 10 kJ mol^{-1} (see Figure 2). A subtraction of the benzene–benzene potential energy from the pmf shows that the solvent contributions to the pmf functions are qualitatively the same (cf. open squares in Figures 1 and 2). In both cases there is a free energy barrier between the close-contact and solvent-separated dimers associated with the solvent where the latter is slightly favored by ca. 3 kJ mol^{-1} (cf. Table I).

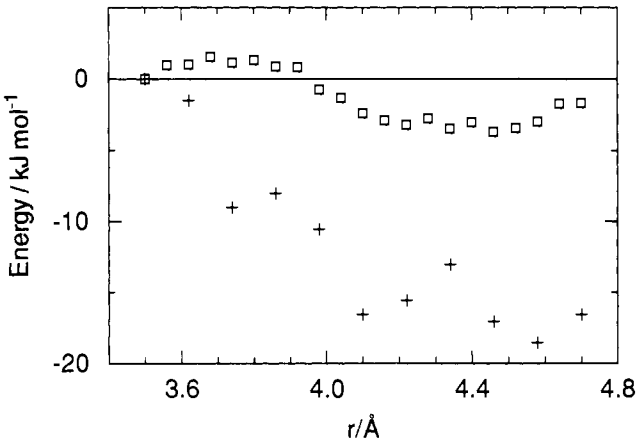

Figure 3. The solvent contribution to the potential of mean force, $w_s(r)$ (open squares), and the ensemble average of the total benzene–water potential energy, U_{BW} (pluses), for a path from the close-contact stacked minimum to the close-contact T-shaped minimum as a function of the benzene–benzene separation (see text for details of the path).

The solvent contribution to the pmf function for the transformation between the two close-contact dimers is displayed in Figure 3. Rather unexpectedly, the difference in free energy originated from the solvent, $w_s(r)$, is very small, only 1.6 ± 1.3 kJ mol^{-1}. Since the T-shaped dimer exposes a 26-Å^2 larger area toward the solvent, conventional hydrophobic interaction theory would predict the stacked dimer to be favored by ca. 5 kJ mol^{-1} (cf. below). This contradiction is resolved by considering the direct benzene–water interaction. Previous investigations[15,17,18] have shown that, whereas the hydration in the benzene plane shows all signs of being hydrophobic, the hydration close to the C_6 axis is slightly different. Although these water molecules (one or at most two on each side of the benzene plane) have an increased tendency of forming hydrogen bonds with the network as compared to bulk water molecules (a characteristic of hydrophobic hydration), these water molecules are also preferentially ordered relative to the benzene molecule by an attractive benzene–water interaction ranging down to −13 kJ mol^{-1}.[15] Since the number of such accessible regions differs between the stacked and T-shaped dimer by one, it is conceivable that the variation of the total benzene–

(29) Note, we are only comparing the free energy of different benzene configurations (points in the configuration hyperspace). At the present stage we cannot unequivocally determine which arrangement is the most frequent one by taking into account the widths of the minima. For such a determination we need in principle a complete knowledge of the pmf as a six-dimensional function. Furthermore, a likely complication in this complete configurational space is the difficulty of dividing the hyperspace unambiguously into well-defined regions corresponding to close-contact stacked dimers, etc. The reason is that these regions are separated with low barriers, or barriers are even absent, in the complete space.

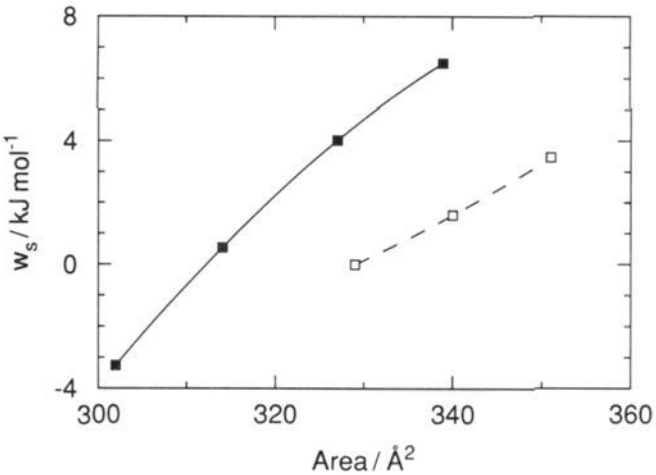

Figure 4. Solvent contribution to the potential of mean force as a function of the area available for hydrating water molecules. The configurations considered are close to the stacked (filled squares) and the T-shaped (open squares) close-contact dimer.

water potential energy, which is included in $w_s(r)$, conceals the change that originates from the reorganization of the water structure. Indeed, Figure 3 shows that the total benzene–water potential energy decreases gradually as the stacked dimer is transformed into the T-shaped one, the total difference being 16 ± 3 kJ mol^{-1}. However, the effect on the free energy is smaller due to entropy compensation from an increased benzene–water structure. Thus, it appears that the increased area exposed toward water by the T-shaped dimer, and the consequently larger free energy cost, is well compensated by the effects of an increased direct benzene–water interaction involving the π-electrons of the benzene molecule.

To conclude this part, we may state that the origin of the lower free energy of the T-shaped dimer as compared to the stacked one arises from the more favorable benzene–benzene *as well as* total benzene–water interactions, both of the order 10 kJ mol^{-1}, which *together* overrule the hydrophobic free energy which is also of the same order but favors the stacked dimer. Hence, without the quadrupole moment, where only the hydrophobic surface free energy would remain, the opposite would have been the case; i.e., the close-contact stacked dimer would have been favored over the close-contact T-shaped one.

A comparison of the pmf and the benzene–benzene potential functions in Figures 1 and 2 shows that the minimum positions of the pmf are shifted inward as compared to the minima of the benzene–benzene potential functions. The hydrophobic free energy per surface area may be obtained by considering the solvent contribution versus the water area available around the benzene dimer for *small* displacements in the neighborhood of the close-contact minima. Figure 4 shows that approximately linear relations are obtained. The hydrophobic surface free energies extracted are 53 mJ m^{-2} (0.29 kJ mol^{-1} Å^{-2}) and 25 mJ m^{-2} (0.14 kJ mol^{-1} Å^{-2}) for the stacked and the T-shaped dimer, respectively. A likely reason for the discrepancy between the two geometries is that the region, where the surface area is varying, is fairly planar in the case of the stacked dimer, whereas this region is more concave for the T-shaped dimer. In the latter case the increase of the surface area with the benzene separation exaggerates the increase of the number of primary hydrated water molecules and, hence, underestimates the hydrophobic free energy. The obtained values are reasonable but larger than that obtained from solubility measurements of alkanes in water, 0.1 kJ mol^{-1} Å^{-2},[30]

The gross features of the solvent contribution to the pmf functions are, of course, a packing effect. This is illustrated in Figures 5 and 6 which show the benzene dimer and the 6 or 10 water molecules that are closest to the midpoint of the benzene

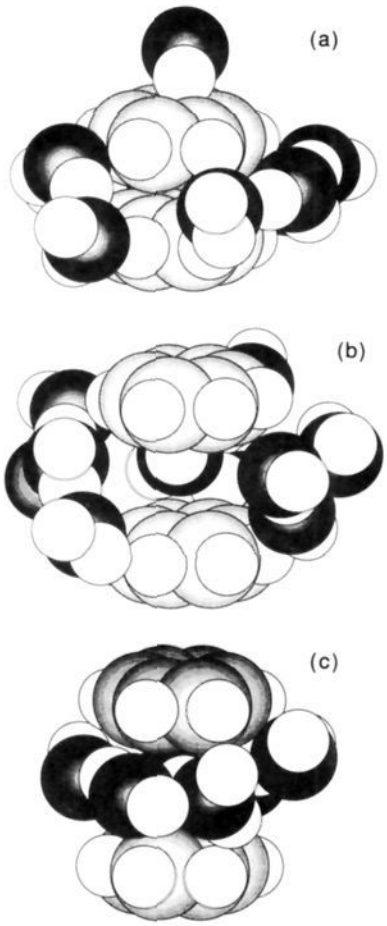

Figure 5. View of water molecules in the neighborhood of the stacked benzene dimer taken from the last simulated configuration. The benzene–benzene separations are r = 3.5 Å (a), r = 5.3 Å (b), and r = 7.1 Å (c) corresponding to the close-contact minimum, the following maximum, and the solvent-separated minimum of the potential of mean force, respectively (cf. Figure 1). For clarity, in (a) and (b) only the 10 and in (c) the 6 water molecules closest to the midpoint of the benzene molecules are displayed. Full van der Waals radii are used (H 1.1, O 1.5, and C 1.7 Å).

molecules. The configurations of the water molecules are taken from the last simulation time step and full van der Waals radii are used. The three selected benzene separations shown correspond to the two minima and the intervening peak of the pmf function. The figures show that the minima indeed correspond to a close-contact dimer and a solvent-separated arrangement with a full hydration layer in between, thus defending the denotation. In particular, the inaccessible void between the dimer at the intermediate distance, corresponding to the barrier peak, is obvious. Moreover, the larger void for the stacked dimer is in accord with its higher solvent induced free energy barrier.

The pmf function for the stacked dimer is qualitatively the same as that theoretically predicted for two hydrophobic solutes in aqueous solution[31] and latter simulated for two Lennard-Jones solutes modelling rare gas atoms[32,33] or methane molecules[34] in water. In these cases the free energy difference between the close-contact and solvent-separated minima was small (<1 kJ mol^{-1}) and the minima were separated by a barrier of 2–3 kJ mol^{-1}. A similar solvent-separated minimum has also been found in model simulation of methane close to a hydrophobic surface.[35] Thus, there is a good qualitatively agreement between the present and

(30) Tanford, C. *The Hydrophobic Effect. Formation of Micelles and Biological Membranes*; Wiley: New York, 1980.

(31) Pratt, L. R.; Chandler, D. *J. Chem. Phys.* **1977**, *67*, 3683.
(32) Pangali, C.; Rao, M.; Berne, B. J. *J. Chem. Phys.* **1979**, *71*, 2975.
(33) Watanabe, K.; Andersen, H. C. *J. Phys. Chem.* **1986**, *90*, 795.
(34) Ravishanker, G.; Mezei, M.; Beveridge, D. L. *Faraday Symp. Chem. Soc.* **1982**, *17*, 79.
(35) Wallqvist, A.; Berne, B. J. *Chem. Phys. Lett.* **1988**, *145*, 26.

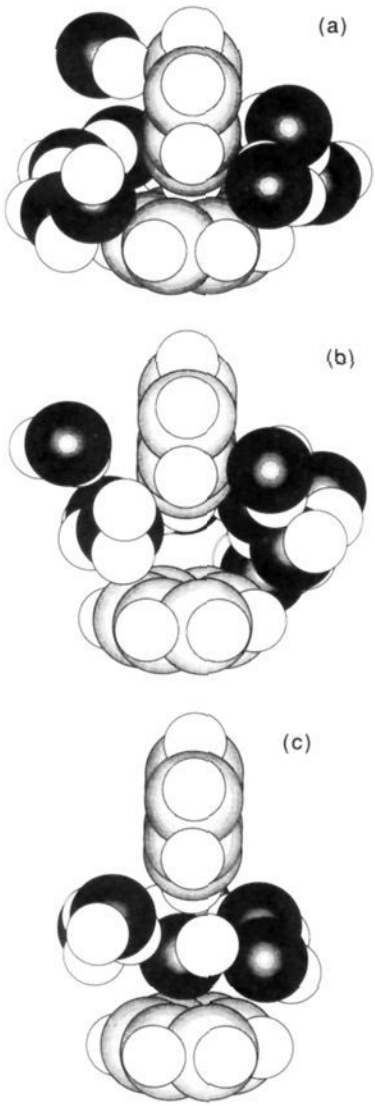

Figure 6. Same as Figure 4, but for the T-shaped benzene dimer. The separations are r = 4.7 Å (a), r = 6.5 Å (b), and r = 8.3 Å (c).

previous investigations of the existence of a well-resolved solvent-separated free energy minimum. The considerably higher energy barrier for the benzene dimer is a direct consequence of the larger cross section.

In the investigation of the *stacked* benzene dimer in aqueous solution Ravishanker and Beveridge[13] obtained essentially a flat and extended minimum of the pmf ranging from r = 4 to 7 Å, ca. 40 kJ mol^{-1} deep. This is completely at variance with the present investigation (cf. Figure 1). As discussed by Jorgensen and Severance,[14] the result by Ravishanker and Beveridge is not realistic, and the reason is likely an insufficient sampling.

Jorgensen and Severance have undertaken an ambitious study where they calculated the pmf function for the benzene dimer in aqueous solution where the pmf is *averaged* over the benzene orientations at each separation.[14] Although it is questionable whether the orientational average is complete,[36] their study shows a number of interesting points. The orientationally averaged pmf function has a broad double minimum with a depth of 4 to 5 kJ mol^{-1} (Figure 6 of ref 14). This depth is compatible with the pmf functions obtained in the present investigation. Furthermore, their minima occur at 5.4 and 7.8 Å and these are separated by a barrier

(36) For example, the statistical uncertainty of the *difference* in the pmf for adjacent points (Δr = 0.2 Å) in Figure 7 of ref 14 is judged to be ≤2 kJ mol^{-1} which is approximately an order of magnitude larger as compared with the present investigation. This large difference in accuracy is mainly due to incomplete orientational averaging in the study of Jorgensen and Severance.

Table II. Assignment of Water Molecules into Classes for the Solvent-Separated Stacked Benzene Dimer (cf. also Figure 7)[a]

name of class	restriction[b]	av no. of water molecules
primary hydration shell	$r_{BW,min} < 6$	48.1 (5)
secondary hydration shell	$6 < r_{BW,min} < 9$	102.0 (3)
bulk	$r_{BW,min} > 9$	349.8 (5)
middle	$\lvert z_W \rvert < 3$ and $\rho_w < 2.5$	1.9 (1)
top[c]	$\theta_W < 30°$ or $\theta_W > 120°$ and $r_{BW} <$ 5.1 as well as $\lvert z_W \rvert > 3$	2.8 (1)
side[c]	$60° < \theta_W < 120°$ and $r_{BW} < 6.3$	31.7 (4)

[a] The upper three entries denote the first set of classes, whereas the lower three the second set where primary hydrated water molecules are further divided into subclasses. The uncertainties given are one standard deviation and are based on a division of the total runs into 3-ps segments. [b] r_{BW} denotes the (center-of-mass) benzene–water separation, $r_{BW,min}$ the smallest of the two benzene–water separations, z_W the z-coordinate of the water molecule (the benzene molecules are placed symmetrically about z = 0, $\rho_W = (x_W^2 + y_W^2)^{1/2}$, and θ_W = arctan (ρ_W/z_W). Distances are given in ångströms. [c] The definitions of the top and side regions agree with those used in ref 15.

of ca. 2 kJ mol^{-1}. The former minimum is likely to be dominated by close-contact T-shaped dimers whereas the latter one could be constituted of solvent-separated stacked dimers. Hence, the resulting rather peculiar orientational averaged pmf function probably originates from the variation of the orientational distribution in order to minimize the free energy at different separations.

The implication of the pmf functions on the relative orientation of aromatic side groups in proteins is not straightforward. In proteins the orientations of these groups are constrained by the backbone chain and the surrounding is often less polar than water. But Figures 1 and 2 show that the depths of the close-contact T-shaped minimum and the two minima of the stacked dimer do not largely deviate from the corresponding values of the *direct* benzene–benzene interaction. Hence, in a less polar medium a reasonable assumption is that the close-contact stacked configuration is still unfavorable, as compared to the T-shaped one. This is in accord with experimental results from the examination of relative orientation of aromatic side groups where the probability of the stacked configuration at contact distance is found to be suppressed.[7,8]

Structure. The hydration of the benzene dimer is (within the statistical uncertainty) in most aspects identical with that of a single hydrated benzene molecule as previously investigated by using the same potentials and external conditions.[15] However, an obvious difference occurs in the benzene–water radial distribution function where the amplitude is reduced at distances comparable to the benzene dimer separation. The integrated deficiency of water molecules is ≈4 which is close to the ratio of the molecular volume of benzene and water, and thus the reduction of the amplitude is a simple exclusion effect.

The largest structural change occurs for water molecules located between the solvent-separated stacked benzene dimer. In order to obtain a more detailed picture of the hydration structure for this benzene arrangement, water molecules are divided into two sets of classes depending on their location. Table II gives the definitions as well as the average number of water molecules in the classes, whereas Figure 7 shows the extension of the middle, top, and side regions.

As previously discussed, the water molecules in the middle region of the solvent-separated stacked benzene dimer are located in a narrow gap and are confined to one layer. Figure 8 shows that the width of the water layer is ≈1.3 Å, and since the middle region is confined by flat end surfaces (cf. Figure 7), the width is not heterogeneously broadened by curved surfaces. The inflection point of the rise of w_s upon reducing the dimer separation from the solvent-separated minimum occurs at 6.0 Å (cf. Figure 1). The use of the width of the water layer at 7.1 Å separation

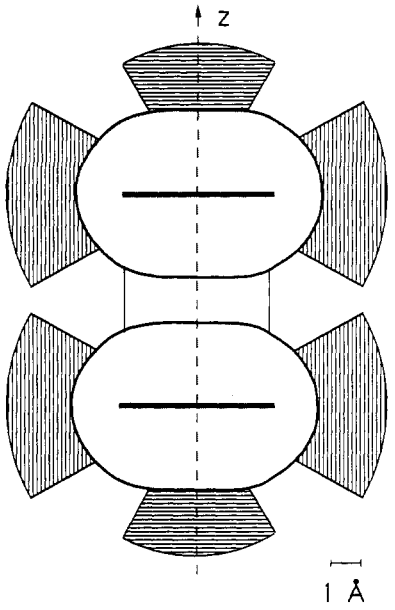

Figure 7. Illustration of the middle (open), top (horizontally dashed), and side (vertically dashed) regions for the solvent-separated stacked benzene dimer. The thick solid lines denote the benzene planes and the shaded area the water excluded region (taken from Figure 2 of ref 11). The definitions of the regions are given in Table II.

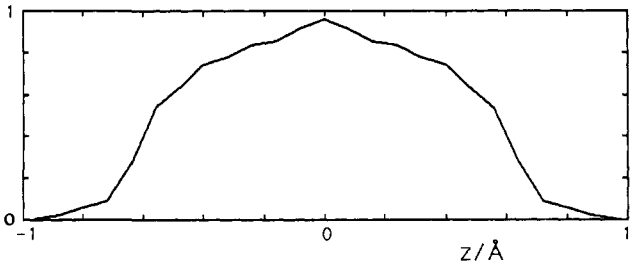

Figure 8. Water density profile parallel to the z-axis for the middle region for the solvent-separated stacked benzene dimer. The averaged standard deviation is 0.06. The curve has been symmetrized and the ordinate is in arbitrary unit.

gives an estimated width of ≈0.2 Å at 6.0 Å separation. This implies that the water layer is strongly compressed before being squeezed out. Moreover, this conclusion is supported by the sharp change of w_s at ≈6 Å, since the rapid change is an effect of water molecules being collectively squeezed out, which is preceded by a compression into a narrow layer.

The preferential orientation of the water molecules in the middle region is examined by means of the distribution function of the z-axis–dipole vector and z-axis–OH-bond vector angles. Since $z = 0$ constitutes a symmetry plane, the angular distribution functions (adf's) possess even symmetry. Figure 9 shows that, at the solvent-separated minimum, some preferential ordering exists but it is reduced as compared with the top region (not shown but similar to Figure 3 of ref 15). In particular, there is a tendency of having one hydrogen pointing along the z-axis, and thus the dipole vector is tilted ≈60° with respect to the z-axis. The lowered preferential orientation in the middle region is corroborated by the less attractive electrostatic interaction for adjacent benzene–water pairs, on the average −1.4 kJ mol^{-1} in the middle region as compared with −2.9 kJ mol^{-1} in the top region.

It has previously been shown that the preferential orientation in the top region is dominated by electrostatic interactions.[15] However, in the middle region the leading electrostatic fields from the quadrupole moments of the two benzene molecules oppose each other. Therefore, the effect of the electrostatic field on the water orientation is reduced. But it is still unclear whether the remaining electrostatic interaction *or* the tendency of optimizing the number of hydrogen bonds to adjacent water molecules in a confined region, as previously demonstrated for hydration of hydrophobic

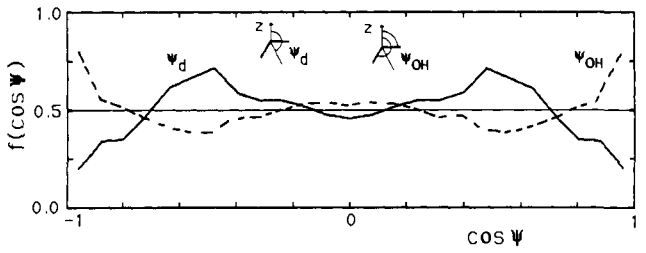

Figure 9. Angular distribution function for z-axis–dipole vector angle (full curve) and the z-axis–OH-bond vector angle (dashed curve) for water molecules belonging to the middle region obtained for the solvent-separated stacked benzene dimer. The averaged standard deviation is 0.11 [f(cos Ψ_d)] and 0.07 [f(cos Ψ_{OH})]. The curves have been symmetrized and the thin solid line refers to isotropic distributions.

Table III. Average Number of Water Neighbors within 3.5 Å from a Water Molecule, n_{NN}, and Average Number of Hydrogen Bonds with Neighbors within 3.5 Å, n_{HB}, for the Solvent-Separated Stacked Benzene Dimer[a]

	hydr shell	bulk	middle	top	side
n_{NN}	4.66 (3)	5.16 (2)	3.94 (8)	4.57 (9)	4.73 (3)
n_{HB}[b]	3.34 (2)	3.37 (1)	2.99 (6)	3.10 (6)	3.38 (2)
n_{HB}[c]	2.23 (3)	2.16 (1)	1.93 (6)	2.03 (5)	2.25 (3)
n_{HB}/n_{NN}[b]	0.72 (1)	0.65 (1)	0.76 (2)	0.68 (2)	0.71 (1)
n_{HB}/n_{NN}[c]	0.48 (1)	0.42 (1)	0.49 (2)	0.44 (1)	0.47 (1)

[a] Two water molecules are considered hydrogen bonded if their pair energy is lower than a threshold value ϵ. Averages are made for molecules belonging to the primary hydration shell, the secondary hydration shell, and bulk as well for molecules belonging to either the middle, top, or side region of the primary hydration shell. Data for the secondary hydration shell are equal to those in bulk and are not given. The uncertainties are one standard deviation and are based on a division of the total runs into 3-ps segments. [b] $\epsilon = -10$ kJ mol^{-1}. [c] $\epsilon = -16$ kJ mol^{-1}.

solutes[37] and at hydrophobic surfaces,[38] is the strongest source to the preferential orientation.

The water structure per se is examined by considering the number of water neighbors and hydrogen bonds as well as by adf's. The presence of solutes introduces trivial changes of the number of hydrogen bonds and neighbors. We will use the ratio of the number of hydrogen bonds to the number of water neighbors as the inherent tendency of forming hydrogen bonds. Typically, this ratio increases for hydrophobic hydrating water molecules,[15,21,38] whereas it decreases for ionic hydrating water molecules.[39] The results given in Table III show that the ratio is increased by 9% in the primary hydration shell as compared to bulk (and to the secondary hydration shell). (Water molecules beyond 9 Å separation from both benzene molecules are referred as bulk.) This enhancement is the same as that found for water molecules in the primary hydration shell of a single benzene molecule.[15] The same analysis applied to the middle, top, and side regions separately shows a slightly stronger tendency of forming hydrogen bonds in the middle region in comparison with the top and side regions (cf. Table III). In particular, the less demanding energy criteria of a hydrogen bond, $\epsilon = -10$ kJ mol^{-1}, show that each water molecules has (on the average) three hydrogen bonds although the molecules are confined to be in a layer.

Figure 10 shows the adf of the interparticle vector–OH-bond vector angle of water neighbors with respect to the location of a reference water molecule in bulk. The hydrogen-bonded network of a tetrahedral type is manifested by the high probabilities of $\Psi_{OH} \approx 0°$, reflecting the situation where the reference molecule acts as an electron donor, and at $\Psi_{OH} \approx 110°$ where it acts as an electron acceptor. The deviation from the distribution in bulk, shown as difference curves, reveals the increased tetrahedral

(37) Geiger, A.; Rahman, A.; Stillinger, F. H. *J. Chem. Phys.* **1979**, *70*, 263.
(38) Lee, C. Y.; McCammon, J. A.; Rossky, P. J. *J. Chem. Phys.* **1984**, *80*, 4448.
(39) Linse, P. *J. Chem. Phys.* **1989**, *90*, 4992.

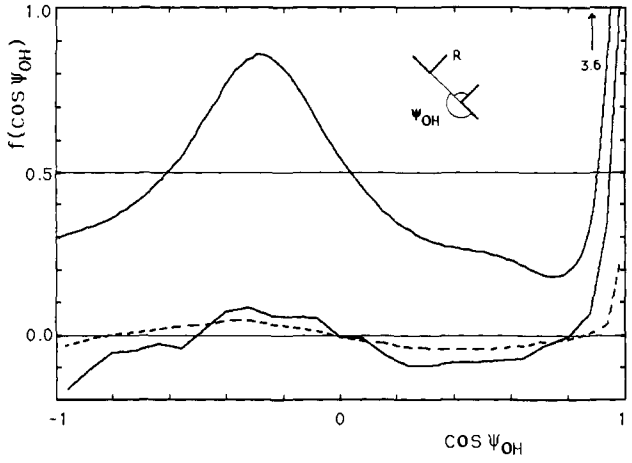

Figure 10. Angular distribution function for interparticle–bond vector angle for water pairs. Averages are made over water neighbors (<3.5 A separation) from reference water molecules (labeled R) belonging to the bulk (upper solid curve), to the middle region of the solvent-separated stacked benzene dimer (lower solid curve), and to the primary hydration shell of a single hydrated benzene molecule (dashed curve) (from ref 15). The bulk adf has been subtracted from the last two adf's. The averaged standard deviation is 0.003 (bulk), 0.04 (middle region), and 0.007 (primary shell of benzene). The thin solid line at 0.5 refers to an isotropic distribution in bulk and same vertical scale applies to all curves.

structure in the middle region. This enhancement is considerably larger than that of the rest of the primary hydration shell of the benzene dimer (not shown) which is equal to that for water molecules in the primary hydration shell of a single benzene molecule (cf. Figure 10).

Thus, the hydration of a stacked benzene is very similar to that of a single hydrated benzene molecule. The radial benzene–water correlation is slightly modified by the excluded volume effect, but the preferential water orientation remains essentially unaffected with the largest exception for water molecules located between the solvent-separated stacked dimer. These water molecules show a weaker preferential orientation with respect to the benzene molecules and an enhanced tetrahedral water structure as compared with the rest of the primary hydration shell.

Summary

Molecular dynamics simulation has been carried out on a model system of an aqueous solution of a benzene dimer. On the basis of thermodynamic perturbation theory, pmf functions for stacked and T-shaped configurations have been calculated. These two arrangements on the six-dimensional hypersurface were selected, since the benzene–water surface is minimized for the stacked arrangement, whereas the direct benzene–benzene interaction is lowest for the T-shaped one.

The investigation with the present limitation, of which the most important is probably the pairwise potential assumption, shows that the close-contact T-shaped dimer has the lowest free energy. The more favorable benzene–benzene and benzene–water interaction prevailing for the T-shaped geometry exceeds the increase in the hydrophobic surface free energy as compared with the close-contact stacked dimer. Since the investigation is limited to pmf functions for two arrangements, it is not yet possible to consider the importance of these arrangements for the association constant. The role of other configurations with favorable benzene–benzene interaction, as the displaced stacked dimer, has first to be assessed.

The stacked dimer possesses a well-defined solvent-separated minimum a few kJ mol^{-1} below the close-contact minimum, and the two minima are separated by a barrier of $\approx$9 kJ mol^{-1}. The existence of a low lying solvent-separated minimum is in accord with simulation studies of aqueous solutions of small apolar solutes. The present result is, however, completely at variance with a similar simulation study of a stacked benzene dimer by Ravishanker and Beveridge,[13] but consistent with the pmf averaged over the benzene orientations by Jorgensen and Severance.[14]

The structure of the primary hydration shell of the benzene dimer is very similar to that of a single hydrated benzene molecule. The main exception occurs for water molecules located between the solvent-separated stacked dimer. These molecules show a weaker preferential orientation with respect to the benzene molecules and an enhanced water structure as compared with the rest of the primary hydration shell.

Acknowledgment. I wish to thank Professor J. Carey for an introduction to the area of aromatic–aromatic interaction in proteins. Generous allocation of computer time on the IBM supercomputer in Skellefteå by Superdatorcentrum Norr (SDCN), as well as financial support from the Swedish Natural Science Research Council (NFR) and from Kungliga Fysiografiska Sällskapet, Lund, is gratefully acknowledged.

Registry No. Benzene, 71-43-2.